

Study of the Engineering Geological Problems of the Havasan Dam, with Emphasis on Clay-Filled Joints in the Right Abutment

Mahdi Rasouli Maleki

Received: 24 January 2011 / Accepted: 17 June 2011 / Published online: 12 July 2011
© Springer-Verlag 2011

Abstract Havasan dam site is located in northwest of Iran. The planned concrete dam is to be built on Cretaceous limestone. Faulted and fractured limestone is exposed at the dam abutments and in the reservoir area. Rock mass properties including the deformation modulus and uniaxial compressive strength were calculated using different rock mass classification systems (RMR, Q, GSI and DMR). Laboratory tests indicate that joint filling materials contain clay with low to high plasticity (CL to CH) and low to medium potential swelling pressures. X-ray diffraction analysis confirms that the reason for potential swelling of joint fillings is the existence of clay minerals (such as illite and montmorillonite). The study results about the shear strength of clay-filled joints show that under JRC–JCS condition (laboratory scale), JRC_n – JCS_n (large scale) and normal stress equal to 0.25–4 MPa, the range of shear strength of clay-filled joints will be equal to 0.2–2.17 and 0.14–1.72 MPa. In some areas dissolution along the joints results in high permeability, especially in the right abutment. Three dominant joint sets occur in the exploration galleries which have been excavated in the right abutment. The maximum aperture of these joints varies from 7 to 9 cm, and the joints are typically filled with clay. Preliminary analysis shows that the presence of open joints which will cause seepage of water, combined with the impact of the clay-filled joints and forces acting on the slopes, could lead to slope failures and rock falls. In addition, the assessment of slope stability results in

abutments using limited equilibrium method and Swedge software under dynamic and static conditions shows that two wedges formed on the slopes of the abutment by the natural joints are potentially unstable. The rock wedge on the left abutment is smaller but presents higher sliding potential. In addition, there is no probability of planar failure due to the geological condition of the dam abutments. This paper summarizes the site investigation and subsequent analysis, which resulted in a recommendation not to construct this site. We offer some potential mitigation plans to consider if a dam were to be built at this site.

Keywords Engineering geology · Clay-filled joints · Swelling pressure · Slope stability · Swedge software

1 Introduction

The proposed site of Havasan dam is located on the Havasan River in northwest of Iran (Fig. 1). This river flows on western slopes of the Zagros mountain range. The dam would supply water to the city of Sar-Pol-Zahab and irrigate the downstream farmlands. It would be constructed under the supervision of the Energy Ministry of Iran. The dam is planned as a double-curvature arch concrete structure 110 m high with a crest of ~150 m and storage capacity of 180 million m³. This paper discusses the engineering geology of the site, with an emphasis on clay-filled joints and their effect on the stability of the abutments. The presence of clay-filled joints poses potential long-term performance problems for the dam. Engineering geologic investigations in dam site involves field and laboratory testing and subsequent stability analysis.

M. R. Maleki (✉)
Engineering Geology and Rock Mechanics Department,
Tunnel Consulting Engineers, Tehran, Iran
e-mail: Mahdi.Rasouli@yahoo.com

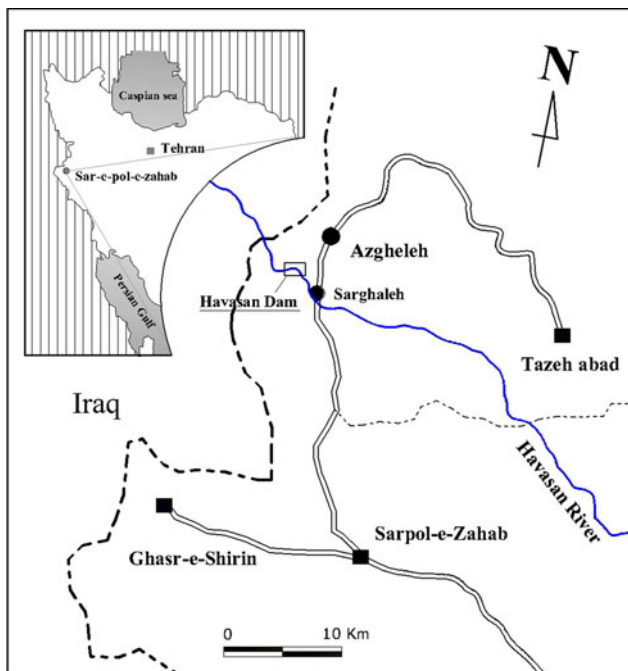


Fig. 1 Location of studied area in Iran

2 Geology of site

A generalized geological map of the project area is illustrated in Fig. 2. This area is located within the folded Zagros Mountain range, which extends northwest from central Iran. The Talezang formation belongs to the Upper Cretaceous limestone and Quaternary deposits crop out over the study area. The Talezang formation consists of thin to medium bedded limestone layers (hard, grey, bio-calcitic packstone) and forms the abutments and foundations of the dam. This formation contains dissolution and karstic features (Fig. 3).

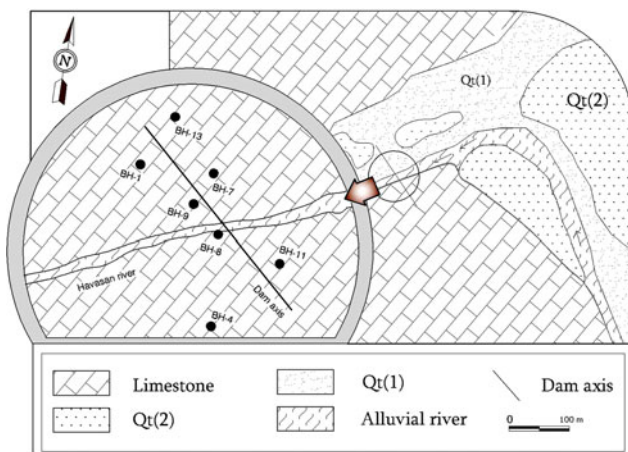


Fig. 2 Geological map of studied area

The proposed dam would be constructed in a V-shaped deep valley. Its axis trends northwest, perpendicular to strike of bedding. The inclination of the slopes is about 50–55°. The approximate direction of bedding in the dam site area is N35E. The dam axis and the Havasan River flow direction in the related site trend N45W and N60E, respectively. The dip-direction of the beddings is parallel to slopes in right abutment; whereas, in the left abutment they slope inward. The upper level of rock formations is covered by alluvial deposits in right abutment; whereas, there are rock outcrops on the left abutment. The bedding strike in the upper part of the right abutment at elevation 530 m changes to N60E due to the movement of fault-F that has moved up the upper side of right abutment.

Based on current design, the elevation of the dam crest is at 560 m, about 30 m over the fault elevation. There are two permanent springs with discharge capacity about 15–20 l/s into the river in upstream and right abutment. Based on the studies and dye tracer it is determined that water from the springs are calcareous and karstic, indicating that the springs can act as conduits for water from the dam reservoir (Fig. 3).

3 Engineering Geological Investigations

Engineering geological investigations mainly include surveying of joints on the outcrop, exploration borings, laboratory and in situ testing.

3.1 Study of Discontinuities and Joints

Description of discontinuities, orientation, spacing, persistence, roughness, aperture and filling were determined in accordance to the ISRM (1981) standard. A total of 406 discontinuities, 128 on the left abutment and 278 on the right abutment have been studied.

The input data from the site investigation were used in Dips 5.1 (Rocscience 2002a) computer software, to determine the dominant fractures for rock units in both abutments (Figs. 4, 5).

The investigation results show that the bedding planes are the dominant discontinuities and control the rock mass properties in both abutments of the dam. Therefore, it could be mentioned that water will seep at higher volume within right abutment where there are more discontinuity sets (about 5 joint sets). So this side of the dam is weaker than left side due to the presence of more joint sets.

3.2 Exploration Borings

For subsurface investigations, seven boreholes with the total length of 514 m were drilled. Moreover, four

Fig. 3 Karstic features in the dam site (a) and discharge point a karstic spring into the river (b)

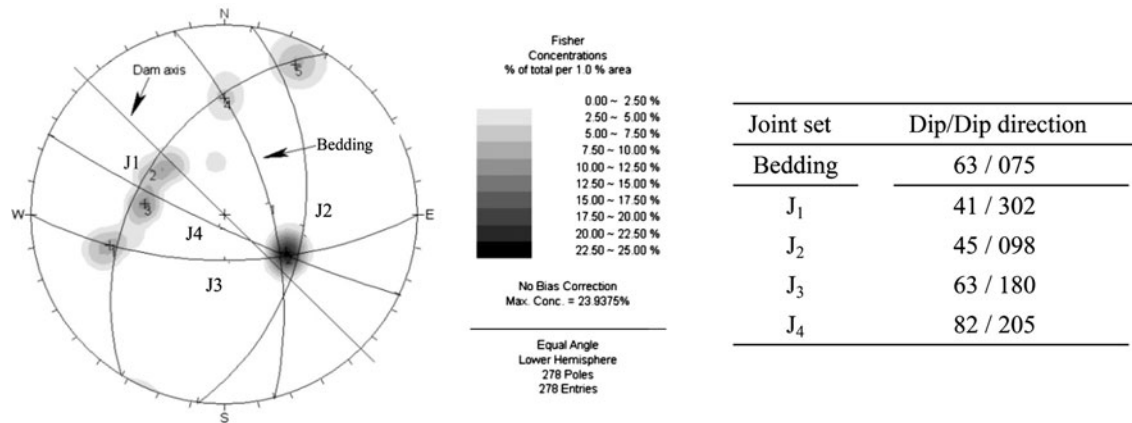
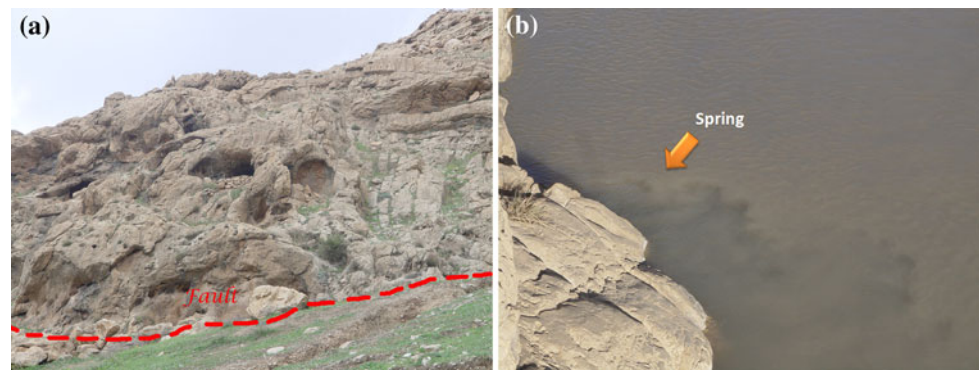


Fig. 4 Polar diagram of discontinuities for *right* abutment

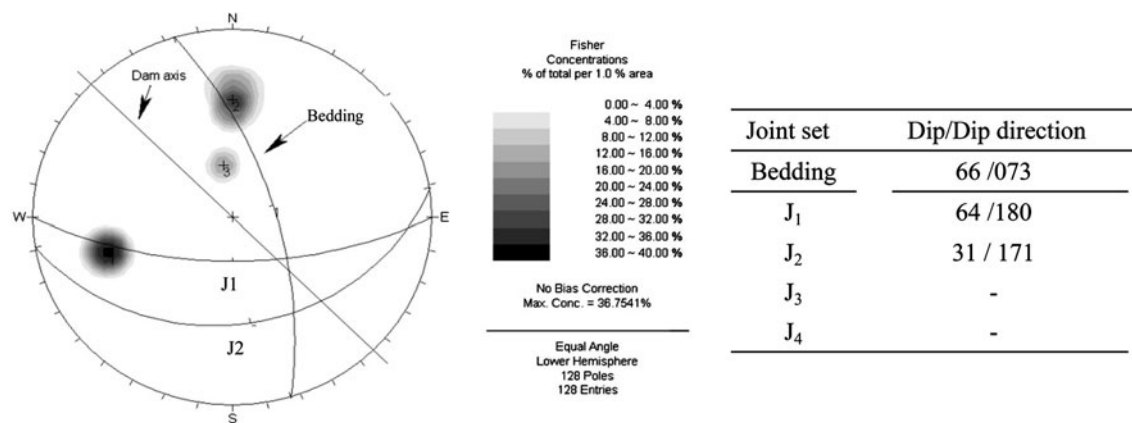


Fig. 5 Polar diagram of discontinuities for *left* abutment

exploration galleries with the length of about 7 m were excavated in the abutments. The geological cross section of the dam is shown in Fig. 6. In addition to the bedding planes, three clay-filled joint sets were observed in the right abutment galleries (Fig. 7). These joints are open and nearly parallel to the slopes. Field investigations of dam site showed that the main source of joint infilling materials is the alluvial deposit on the surface of the right abutment. Geometrical characteristics of clay-filled joints in the right

abutment are shown in Table 1. The geological cross section is given in Fig. 6.

3.3 Permeability of Rock Mass

The major controlling factor for estimating the water loss from the dam reservoir is the permeability of rock masses at the dam site. This factor varies depending on the geomechanical conditions of the site. However, during the

Fig. 6 Geological cross section and location of boreholes along the dam axis

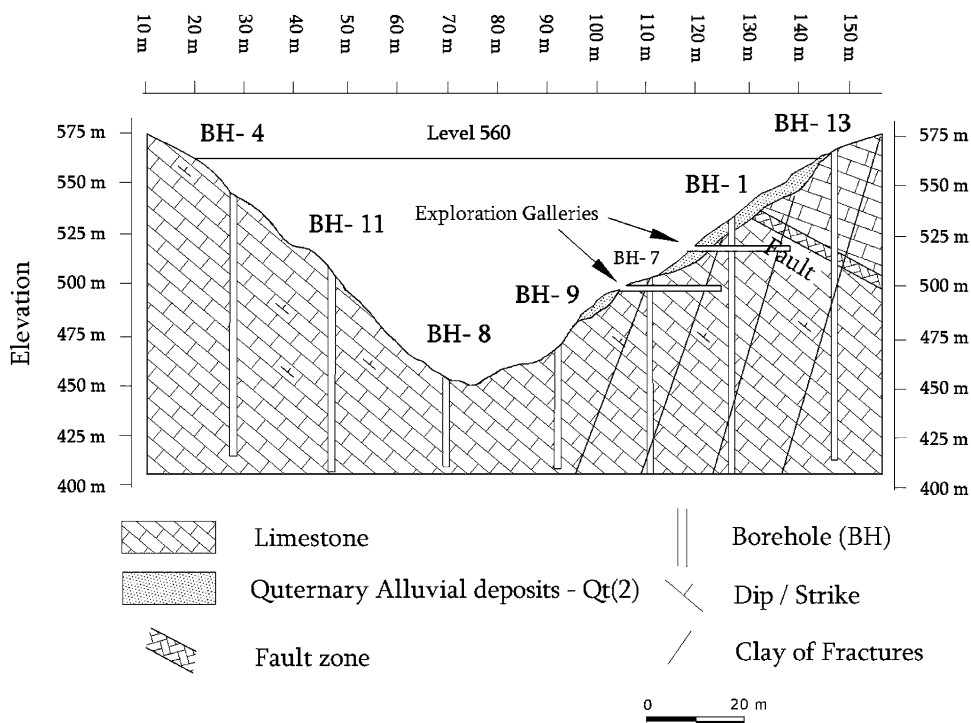


Fig. 7 The presence of clay-filled joints in right abutment of the dam



exploration phase water pressure tests (Lugeon) have been performed in the seven boreholes. The results show Lugeon values vary from 1 to 100. Due to joint sets and fractures induced by faulting and karstic features, the permeability of rock masses in right abutment is higher than the left one. Therefore, the right abutment has the potential for high water seepage. In Table 2 the results of Lugeon tests for the boreholes are summarized and the variations of measured Lugeon values at various depths are shown in Fig. 8.

4 Engineering Classification of Rock Masses

The RMR classification system of Bieniawski (1989) and the Q by Barton et al. (1974) were developed for characterizing the rock mass. These systems have evolved over the years due to reaching a better understanding of the

Table 1 Clay-filled joints properties in right abutment of the dam

No	Dip/dip direction	Separation (mm)	Spacing (m)	Distance to span of gallery (m)
F ₁	76/179	75	1.5	1.8
F ₂	85/183	70	2.2	4.1
F ₃	83/189	91	1.4	5.4

different parameters on the rock mass behavior. The following six parameters are used to classify rock mass by the RMR system:

(1) Uniaxial compressive strength, (2) Rock quality designation (RQD), (3) Spacing of discontinuities, (4) Condition of discontinuities, (5) Groundwater conditions and (6) Orientation of discontinuities.

The value of RMR is:

$$\text{RMR} = (1) + (2) + (3) + (4) + (5) + (-6) \quad (1)$$

Table 2 Lugeon values and frequency of tests in Havasan Dam site

Borehole	Location	Ground water level (m)	No of tests	Lugeon range		Average of Lugeon	Permeability (m/s)
				Min	Max		
BH-1	Right	58.3	17	33	100	58	6.03E-05
BH-7	Right (karstic area)	17.7	5	100	100	100	0.000103
BH-9	Right	34.1	9	46	100	94	9.72E-05
BH-13	Right	81.4	16	5	100	25	2.61E-05
BH-4	Left	112.3	10	1	100	76	7.86E-05
BH-8	Left	18.2	7	1	100	54	5.63E-05
BH-11	Left	52.5	17	1	100	58	5.99E-05

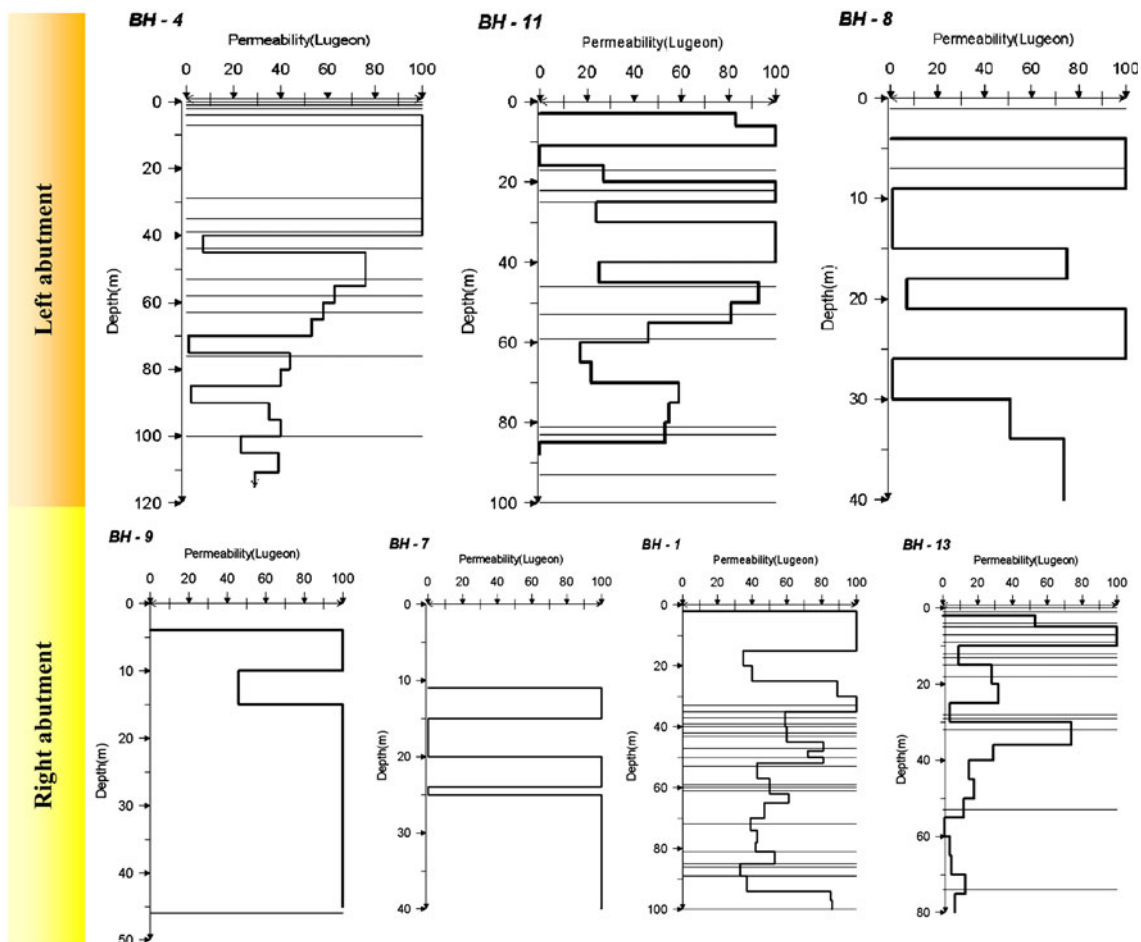


Fig. 8 Variations of Lugeon values with depth of boreholes

The Q or NGI (Norwegian Geotechnical Institute) classification system was developed by Barton et al. (1974), primarily for tunnel design work. The numerical value of the index Q varies from 0.001 to 1,000 and is defined by:

$$Q = \frac{RQD}{J_n} \times \frac{J_r}{J_a} \times \frac{J_w}{SRF} \tag{2}$$

where RQD stands for Rock Quality Designation, J_n stands for joint set number, J_r stands for joint roughness number, J_a stands for joint alteration number, J_w stands for joint water reduction factor and SRF stands for stress reduction factor.

The Geological Strength Index (GSI) was introduced by (Hoek and Brown 1980) and extended by Hoek et al. (1998).

Table 3 Adjusting factors for the dam stability R_{STA} , according to joints orientation for arch of dam (Romana 2003)

Type of dam	Very favorable	Favorable	Fair	Unfavorable	Very unfavorable
Arch	30–60 DS	10–30 DS	30–60 US, 60–90 A	10–30 US	0–10 A
R_{STA}	0	–2	–7	–15	–25

DS dip downstream/US dip upstream/A any dip

Table 4 Correlation between the value of DMR_{STA} and the degree of safety of the dam

DMR_{STA} value	Status
$DMR_{STA} > 60$	No primary concern
$60 > DMR_{STA} > 30$	Concern
$30 > DMR_{STA}$	Serious concern

Dam Mass Rating (DMR) classification system was proposed by Manual Romana (2003) for the foundation of dams. This classification system is used for slope stability, deep excavation, grouting, and anisotropy analysis and determining elasticity of rock. This system includes the following three parameters of rock mass:

(1) Parameter of RMR_{BD} , (2) Correction Factor (CF) and (3) Stability of dam against sliding.

Snell and Knigh (1991) developed a systematic approach for the problem of dam stability taking into account all the forces and stresses acting on the dams. Based on their study it appears that a different set of adjusting factors must be applied. Table 3 shows the new proposed adjusting factors according to the main discontinuity orientations. The numerical rating values proposed originally by Bieniawski have been retained.

The value of DMR_{STA} is:

$$DMR_{STA} = RMR_{BD} + CF. R_{STA} \quad (3)$$

Table 5 RMR rating for right and left abutment

No	Parameters, rating	Right abutment	Left abutment
1	UCS (MPa)	62.5	52.1
2	RQD (%)	56	51
3	Spacing of discontinuities (mm)	50–200	60–200
4	Joint condition	Persistence: 2–9 m, aperture: >5 mm, surfaces are generally rough, filling materials: soft filling >5 mm and slight weathered walls	Persistence: 2–10 m, aperture: >5 mm, surfaces are slightly rough, filling materials: soft filling >5 mm and moderately weathered walls
5	Groundwater	Damp	Damp
6	Rating adjustment for fracture orientation	–25	0
	RMR	25	46
	Rock mass classes (description)	Poor	Fair

The correlation between the value of DMR_{STA} and the safety of the dam due to sliding or, in other words, the suggested potential risk of dam stability is summarized in Table 4.

These classification systems were used to evaluate the rock mass parameters in the abutments of the Havasan dam and the results are presented in Tables 5 and 6. The results of RMR and Q classification systems confirm the weak rocks existence in the abutments of the dam. In addition, the DMR classification shows some potential problems would be expected in the foundation of the dam and it should be improved.

5 Estimating Rock Mass Parameters

To obtain the deformation modulus and shear strength properties of the rock types at the dam site, some in situ and laboratory tests were carried out. The preliminary results of the laboratory tests are shown in Table 7. Moreover, to estimate design parameters, geomechanic classification systems were used, which will be explained in the following section.

5.1 Compressive Strength and Deformation Modulus of Rock Masses (E_{mass})

The presence of a high quality and strong rock mass in abutments is one of the necessities for construction of

Table 6 Classification of rock masses based on RMR, Q , GSI and DMR systems

Abutment	RMR	Q	Q_c	Q_n	GSI	DMR			
						RMR _{BD}	CF	R_{STA}	DMR _{STA}
Right	25	0.65	0.41	0.26	43–48	50	2.91	0	50
Left	46	1.34	0.7	0.57	39–44	46	2.75	0	46

Table 7 Physical and mechanical properties of the rock units in the abutments of the dam

Parameters (unit)	Right abutment	Left abutment
Unit weight (kN/m ³)	26.81	26.70
Dry unit weight (kN/m ³)	26.29	26.05
Saturated unit weight (kN/m ³)	26.44	26.22
Specific gravity	2.67	2.65
Water absorption (%)	0.20	0.25
Poisson’s ratio	0.18	0.19
E (GPa)	9.5	9
Porosity (%)	1.6	1.7
Uniaxial compressive strength, UCS (MPa)	62.5	52.1
Schmidt hammer	46	41
Cohesion (MPa)	0.18	0.25
Internal friction (°)	24	29

Table 8 Calculated strength values (σ_{cmass}) obtained from different equations

Abutment	Bhasin and Grimstad (1996) (MPa)	Barton (2000) (MPa)	Singh et al. (1997) (MPa)	Average (MPa)
Right	2.24	9.78	16.01	9.34
Left	7.9	11.62	20.22	13.25

Table 9 Calculated deformation modulus values (E_{mass}) obtained from different empirical methods

Abutment	Serafim and Pereira (1983) (GPa)	Grimstad and Barton (1993) (GPa)	Mitri et al. (1994) (GPa)	Hoek and Brown (1998) (GPa)	Read et al. (1999) (GPa)	Average (GPa)
Right	2.37	–	5.46	7.25	1.56	4.16
Left	7.94	3.17	5.74	4.43	9.73	6.21

Table 10 Shear strength parameters calculated based on RMR classification

Abutment	RMR value	Angle of internal friction (°)	Cohesion (MPa)
Right	25	17.5	0.13
Left	46	28.0	0.23

concrete dams. Thus, the rock mass classification systems were used to evaluate the rock mass strength at the dam abutments. There are different approaches for evaluating rock mass strength. The results of calculated σ_{cmass} and E_{cmass} values based on proposed formulas

by various researchers are given in Tables 8 and 9, respectively.

5.2 Estimation of the Shear Strength Parameters

The angle of internal friction and cohesion are the most important part of shear strength parameters of the rock mass. For this study, shear strength parameters of the abutments were estimated by the methods suggested by Bieniawski (1989) as follows:

$$\begin{aligned} \varphi &= 0.5RMR + 5 \\ c &= 0.05RMR \text{ (MPa)} \end{aligned} \tag{4}$$

The calculated angle of internal friction and cohesion values are given in Table 10.

Table 11 Atterberg limits obtained for clay samples taken from joints on right abutment

Sample	LL	Slope of flow line	PI	PI
F1	40.2	0.18	27	13.7
F2	42.5	0.25	28.3	14.2
F3	53.3	0.26	37.4	15.9

6 Filling Materials in Joints

The presence of clay minerals in the rock joints in the foundation and dam abutments could lead to significant loss of water from the reservoir, decreasing the shear strength parameters of joints, creating the swelling pressure in the joint walls, and in general destabilizing the slopes. Clay infillings could be considered as one of the main threats to dam stability. In order to study the behavior of clay infilling of the joints in Havasan dam abutments several samples were tested in laboratory and the results are discussed in the following.

6.1 Atterberg Limits

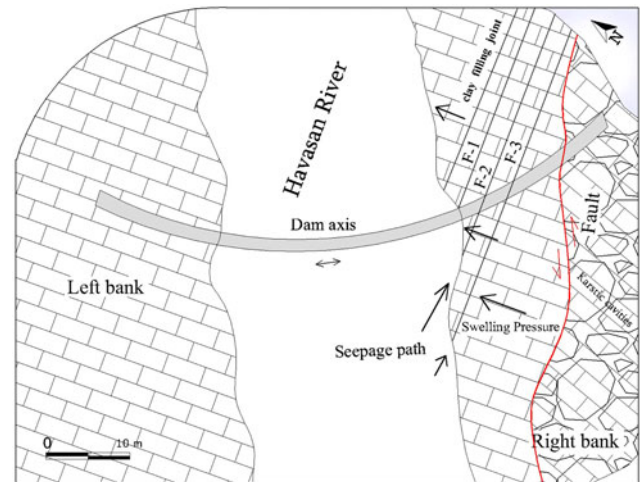
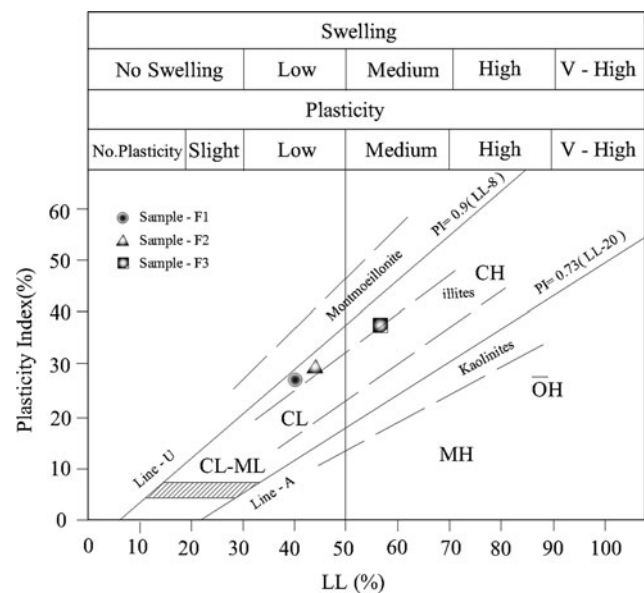
Several samples of the joint filling material were taken from the site and tested in laboratory. According to the Unified Soil Classification System (USCS), the samples present low plasticity (CL) in F1 and F2 joint sets and high plasticity (CH) in F3 joint set. The data also indicate that maximum plastic and liquid limits for the infilling material for F3 set are 53.3 and 15.9% respectively. Atterberg limits and plasticity index of different samples are represented in Table 11.

6.2 Swelling Potential

Swelling is a term generally applied to the ability of a soil to undergo large changes in volume due to increased water content. The main objective of performing swelling tests was to study the behavior of clay-filled joints and their effects on dam structure. Laboratory test results show that the maximum swelling strain is about 0.19% which is equivalent to 5.32 kPa swelling pressure on walls.

The swelling pressure will decrease the shear strength of joints and lead to instabilities of rock blocks on the abutment. As a result, slope failures can destabilize the foundation of the dam and result in rock falls, which will fill the reservoir and also cause massive waves which are able to cause wash outs and uncontrolled overflow spills (Fig. 9).

The plot of the soils on Casagrande's plasticity chart indicates that the clay filling of joints is mainly: CL, low

**Fig. 9** Condition of swelling pressures into direction of abutments and dam axis**Fig. 10** Plasticity chart showing the position of soil in the abutment (Ramana 1993)

swelling/low plasticity and CH, medium swelling/medium plasticity. Soil data plotted confirms the presence and abundance of illite and montmorillonite clays (Fig. 10).

The swell potential of the clay filling in fractures was also evaluated by using the following methods:

- Seed et al. (1962) proposed Eq. 5 for determining the swell potential based on plasticity index, as:

$$S = (21.16 \times 10^{-3}) \times (PI)^{2.44} \quad (5)$$

- Ola (1982) and Ramana (1993) proposed the swell potential based on plasticity limit and liquid limit as outlined in Table 12.

Table 12 Classification of swelling potential of the clay-filled joint sets

	Description	Seed et al. 1962, S	Ola (1982), PI	Ramana (1993), LL
Potential expansiveness	Low	0–1.5	0–15	<50
	Medium	1.5–5.0	15–25	50–70
	High	5.0–25.0	25–35	71–90
	Very high	<25.0	>35	>90
Joints	F ₁	Low	Low	Low
	F ₂	Low	Low	Low
	F ₃	Medium	Medium	Medium

These results indicate soil of low to medium swelling potentials (see Table 12). The results are in agreement with the earlier deduction of soil being rich in illite and montmorillonite minerals.

6.3 X-ray Diffraction Tests

Since the quality and behavior of soils are functions of clay mineralogy, X-ray diffraction tests were carried out on clay materials in three joint sets. The results indicate that clay minerals (illite and montmorillonite) are the main cause of swelling of clay-filled joints. This phenomenon controls the rock mass behavior in the dam site.

7 Shear Strength of Clay-Filled Joints

The shear strength of joint surfaces in a rock mass is a difficult parameter to determine and is affected by a number of factors. Therefore, it could be mentioned that shear strength of jointed rock mass depends on the type and origin of discontinuity, hardness, roughness, depth of weathering, water and type of filled material.

Considering that all the rock masses contain joints and fractures, the behavior of the rock mass is controlled by sliding on the discontinuities. It is necessary to understand the factors controlling the shear strength of the discontinuities which separate the blocks. According to researches, there are three important factors determining the shear strength of joints in rock:

1. The joint roughness (JRC)
2. The joint wall compressive strength (JCS)
3. The basic friction angle of the rock material.

7.1 Joint Roughness Coefficient

The joint roughness coefficient (JRC) is the key parameter for the empirical estimation of the joint shear strength, especially in the case of interlocked fractures and unfilled

joints. The empirical approach proposed by Barton and Choubey (1977) is the most widely used approach. JRC is a number varying in the interval 0–20 and represents the relevance of roughness in defining the rock shear strength (smooth surface: JCR = 0; very rough surface: JCR = 20). In summary, JRC could be estimated by:

1. Comparing the real profile of the asperities with standard profiles (JRC₀).
2. Performing a Tilt Test.
3. Measuring length and amplitude of the asperity profile and using a graphic correlation with JRC using the following equation:

$$JRC_n = JRC_0(L_n/L_0)^{-0.02JRC_0} \quad (6)$$

where L_n represents the larger scale length and L_0 is the laboratory scale length, i.e., 100 mm.

7.2 Joint Wall Compressive Strength

The joint wall compressive strength (JCS) is of importance to the shear behavior of rock joints and in the determination of rock slope stability since it is largely the thin layer of rock adjacent to the joint wall that controls the shear strength. JCS could be estimated by:

1. Comparing the alteration degree of the joint with the degree of alteration of the rock.
2. Performing on site measurements with the Schmidt hammer rebound (L-type) on the most prominent joint surfaces. The value of JCS could be obtained from the Schmidt hammer rebound value (r) as follows:

$$JCS = 10^{(0.00088r\gamma+1.01)} \quad (\text{MPa}) \quad (7)$$

where r is the rebound number and γ is the dry density of rocks.

For larger blocks or joint lengths (L_n), the value of JCS reduces to joint wall compressive strength at a large scale (JCS_n), where the two are related by the following equation:

Fig. 11 Marked range of JRC value of clay-filled joint on the standard profiles

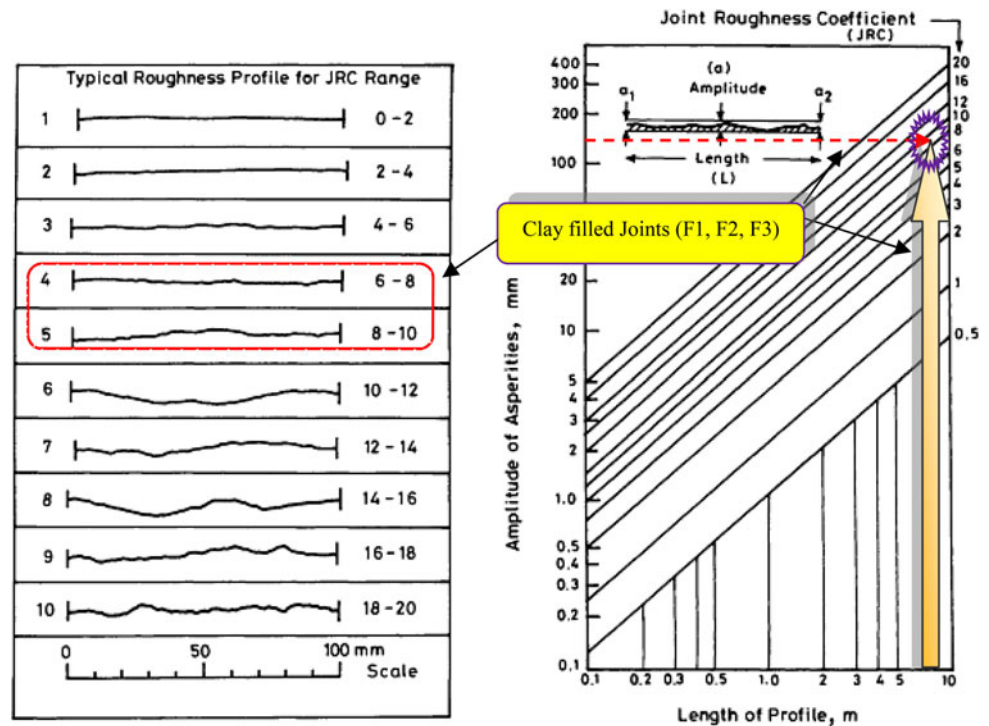


Table 13 Calculated JRC and JCS values of clay-filled joint based on laboratory and field methods

Sample	Input parameters				Calculated parameters				
	L_n (m)	L (m)	γ (kN/m ³)	Schmidt hammer rebound (r)	JRC	JRC _n	JCS _n (MPa)	JCS _n (MPa)	(Jaeger and Cookm 1969) (°)
F1	41	0.8	26.3	42.0	8.0	4.3	12.8	2.8	8.5
F2	43	0.8	26.3	44.0	7.0	4.0	12.9	2.8	6.3
F3	49	0.8	26.3	40.0	9.0	4.3	12.7	2.7	6.6

$$JCS_n = JCS_0(L_n/L_0)^{-0.03JCS_0} \quad (\text{MPa}) \quad (8)$$

In this research, it has been attempted to determine JRC and JCS values of clay-filled joints based on both laboratory and large-scale methods. Figure 11 shows ranges of JRC values of clay-filled joints on the standard profiles.

7.3 The Angle of Internal Friction

The residual friction angle (φ_r) of a joint is a very important component of its total shear strength whether the joint is rock-to-rock interlocked or clay filled. In the (Barton and Bandis 1990) joint model it is proposed to add an angle of primary roughness to obtain the field value of the peak friction angle for a natural joint (φ_j) without filling.

$$\varphi_j = \varphi_r + i + \text{JRC} \log_{10}(\text{JCS}/\sigma) (70^\circ); \text{ for } \sigma/\text{JCS} < 0.3 \quad (9)$$

where φ_r is the residual friction angle; JRC is the accounts for secondary roughness in laboratory tests; JCS is the joint wall compressive strength and i is the angle of primary roughness (undulations) of natural joint surface.

In addition, according to studies done by Jaeger and Cookm (1969), for clay-coated joints the sliding angle of friction is found to be:

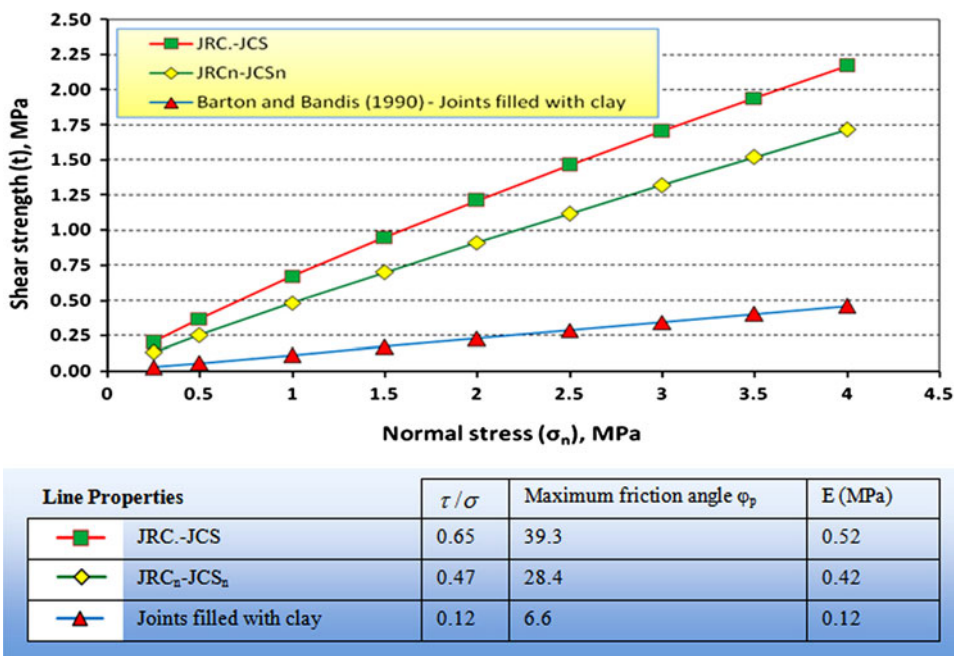
$$\varphi_j = \tan^{-1}(J_r/J_a) \geq 14^\circ. \quad (10)$$

The results obtained show that JRC (laboratory scale) and JRC_n (large scale) for clay-filled joints of the right abutment of the Havasan dam are in the range 7–9 and 4–4.3 respectively. Also JCS (laboratory scale) and JCS_n (large scale) values are respectively in the range 12.7–12.9 and 2.7–2.8 MPa (Table 13). In addition, the sliding friction angle of clay-filled joints is in the range 6.3–8.5 degree.

Table 14 Peak friction angle of joint surface and shear strength values obtained for clay-filled joints

JRC–JCS (lab scale)			JRC _n –JCS _n (field scale)		Barton and Bandis 1990, joints filled with clay Shear strength (τ), (MPa)
Normal stress (σ _n), (MPa)	Peak friction angle of joint surface (°)	Shear strength (τ), (MPa)	Peak friction angle of joint surface (°)	Shear strength (τ), (MPa)	
0.25	15.3	0.20	4.4	0.14	0.03
0.5	12.6	0.37	3.1	0.26	0.06
1.0	9.9	0.67	1.8	0.48	0.12
1.5	8.3	0.95	1.1	0.70	0.17
2.0	7.2	1.21	0.5	0.91	0.23
2.5	6.3	1.46	0.1	1.12	0.29
3.0	5.6	1.71	0.0	1.32	0.35
3.5	5.0	1.94	0.0	1.52	0.40
4.0	4.5	2.17	0.0	1.72	0.46

Fig. 12 Diagram of shear strength–normal stress, maximum friction angle and elastic modulus values of clay-filled joints



7.4 Shear Strength of Joints

Various methods have been proposed for estimating the shear strength of discontinuities. In summary, we have the following equations:

1. Linear Mohr–Coulomb failure envelope with y-intercept (known as cohesion) and slope (known as coefficient of friction, tanφ):

$$\tau = c + \sigma_n \tan \phi \tag{11}$$

where τ = shear strength along the discontinuity; σ_n = effective normal stress acting on the discontinuity; c = cohesion (generally equal to zero or a very small value for clean rock fractures); φ = friction angle.

2. General nonlinear, power-curve model:

$$\tau = c + a(\sigma_n)^b \tag{12}$$

where τ = shear strength along the discontinuity; σ_n = effective normal stress acting on the discontinuity; a, b, c = power-curve parameters.

3. The JRC model (a nonlinear model):

Barton and Choubey (1977) have proposed the following non-linear correlation for shear strength of natural joints:

$$\tau = \sigma_n \tan[\text{JRC} \log_{10}(\text{JCS}/\sigma_n) + \phi_b] \tag{13}$$

where τ = shear strength along the discontinuity; σ_n = effective normal stress acting on the discontinuity; JRC = joint roughness coefficient (typical values: 2–6); JCS = joint-wall compressive strength; ϕ_b = base friction angle (i.e., for saw-cut, smooth surfaces).

The peak friction angle of the joint surface could be obtained from contribution of roughness and hardness of the joint surface:

$$[\text{JRC} \log_{10}(\text{JCS}/\sigma_n)] \quad (14)$$

For joints filled with clay, the following correlation of shear strength is used for low normal stresses (Barton and Bandis 1990).

$$\tau = \sigma(J_r/J_a) \quad (\text{MPa}) \quad (15)$$

In this study, values of shear strength and peak friction angle of clay-filled joint surfaces have been calculated for both JRC–JCS (laboratory scale) and JRC_n – JCS_n (large scale). The result shows that under condition of JRC–JCS and JRC_n – JCS_n and normal stress equal to 0.25–4 MPa, the range of shear strength of clay-filled joints will be equal to 0.2–2.17 and 0.14–1.72 MPa (Table 14). Therefore, it could be concluded that for both JRC–JCS and JRC_n – JCS_n the angle of shear strength–normal stress will be equal to 39.3 and 28.4° respectively (Fig. 12).

Furthermore, the shear strength for joints filled with clay using the formula proposed by Barton and Bandis (1990) it shows that due to presence of clay in joints, the value of the shear strength reduces 0.03–0.46 MPa. In this condition, is reasonable to assume the internal friction angle of clay-filled joints equal to 6.6° for Havasan dam site.

8 Stability Analysis of the Dam Abutments

In the selection and design of a site for dams, the assessment of the abutment stability is very important and often is based on

the limit equilibrium method of the potentially unstable rock blocks. Different computer codes have been developed for this purpose (Rasouli Maleki 2011). In the following, the commercial code Swedge (Rocscience 2002b) has been used.

8.1 Stability Analysis Using Kinematical Method

A kinematic test of both the abutments is shown in Fig. 13 and is used to establish possible failure modes. A daylight envelope and friction angle cone, corresponding to the angle of shearing resistance, is also drawn on the stereonet. The slopes of the left and right abutments are 28 and 17.5°, respectively. The analysis of the joint sets intersecting the slopes shows that there are some joints which are sub-parallel to the slope and have potential for plane failure; while other joints could form wedges and daylight at out of the slope. Based on limit equilibrium method, the condition for sliding of planes or wedges is the time is when inclination of joint surface or intersection line of joint sets of a wedge is greater than the friction angle.

A review of the stereonet of both abutments shows that several wedges were formed by various joint sets. Based on the limit equilibrium method, the stability analysis of dam abutments shows the potential of failure as (Rasouli Maleki 2010):

1. Wedge failure

- In the right abutment, some large wedges with potential northern and northeastern sliding trends can be formed (wedges A, B and C). In this abutment, only the wedge resulted from intersection of bedding plane with joint set 1 (wedge A) is unstable and has sliding potential along the trend calculated at 25/358 (dip/dip direction).
- In the left abutment, wedges formed by intersection of bedding plane with joint set 1 (wedge A) have the probability of sliding. Dip and dip direction of sliding is calculated to be 53 and 126 respectively.

Fig. 13 Kinematics check and simple stability assessment of: (a) on the *right* abutment slope and (b) on the *left* abutment slope

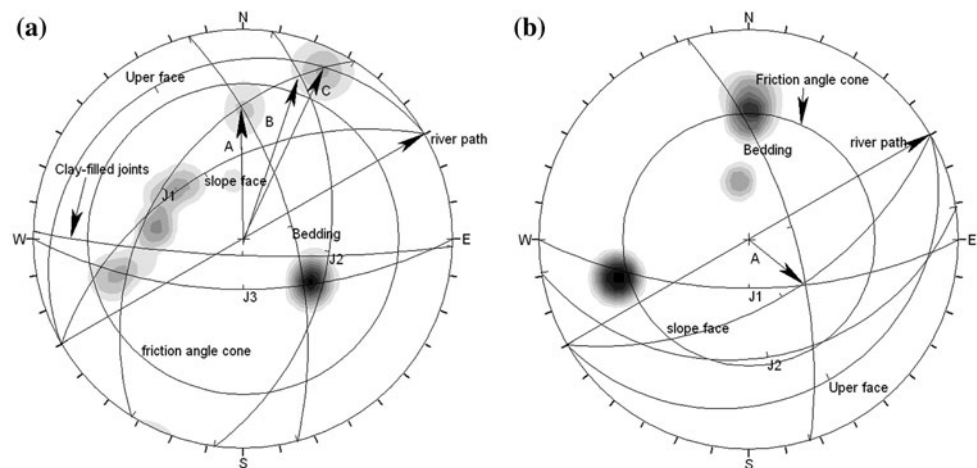


Table 15 Main input parameters

	Parameters	Right abutment	Left abutment
Slope	Dip/dip direction (deg)	50/330	55/150
	Slope height (m)	122	125
	Rock unit weight (kN/m ³)	26.4	26.2
Upper face data	Dip/dip direction (deg)	10/330	15/150
Seismic	Horizontal acceleration	0.15 g	0.15 g

Overall, the stability analysis shows that the created wedges on both the abutments are different in dimensions but similar in trend of sliding and are prone to move downstream.

2. Planar failure

The stereonet plots and related analysis show that there is no potential for planar sliding/failure in the abutments owing to the following reasons:

The joints and bedding direction are not parallel or sub-parallel to the abutment slopes.

1. For the right abutment, the dip direction of bedding is the opposite of that of the slope; in other words, the reversed dip of bedding is corresponding to slope dip.
2. In the left abutment, although the joints and bedding dip direction are in agreement with the slope, due to the higher dip of beddings compared to slope dip, there is no chance of planar failure.

8.2 Stability Analysis Using Swedge Software

The computer software, Swedge (Rocscience 2002a), has the capability to assess the slope stability based on deterministic and probabilistic methods. The input parameters include slope parameters (angle, height, face and unit weight), joint sets, geometry of the upper surface, location/angle of tension crack, water pressure, and seismic forces. In this software, the water pressure distribution model has been selected as filled fissures and the seismic horizontal acceleration has been set 0.15 g which is the value of the potential acceleration extracted from the seismic/earthquake maps of the region for the dam site. The stability analysis of the Havasan dam slopes was performed by the deterministic model under two conditions: (1) dynamic with application of earthquake load, and (2) static without the earthquake loading and with different levels of water pressure in joints. The analysis was performed for all joint sets of dam abutments. The main input parameters used in the analysis are given in Table 15.

The results show that the bedding intersection with joint set 1 could lead to formation of wedges in the abutments of dam. The characteristics of intersection line of joints and sliding trend of wedges in both abutments are shown in Table 16.

Investigation of the effect of clay-filled joints in the formation of unstable wedges indicates that the presence of these joints in the right abutment could not lead to the formation of unstable wedges. The main output parameters in the S-wedge software for analysis of wedges are given in Table 17.

The results shown in Table 17 indicate that the wedges in the left abutment have smaller volume and dimension than those on the right abutment. Accordingly the sliding potential is higher for the wedges on the left abutment. The estimated values of Safety factor (FOS) for blocks on both abutments under dynamic and static conditions and the different levels of water pressure in joints are listed in Table 18 (Rasouli Maleki 2010).

Table 18 shows that the wedge formed on the right abutment will be unstable and will slide if water level rises inside the joints. Maximum and minimum values of the calculated safety factor for the wedge of right abutment, under earthquake load, ranges from 1.25 for dry condition to 0.89 for saturated condition respectively. Consequently, the left abutment has decreased resisting forces and increased driving forces due to the low weight and small wedge. Considering such characteristics, while the water level is 50% higher than the length of joints, the wedge will be unstable under both dynamic and static conditions.

9 Discussion on Selection Criteria for Dam Site

Geological engineering site evaluation for a given project requires an objective assessment of the ground conditions for both the construction and service life of the structure. Initial site selection for dam construction projects is primarily based on ground topography. The selected site should be investigated for potential problems during the construction and long-term stability. In some cases, evaluations support the site selection and offer possible modifications or ground improvement to meet the performance criteria of the dam, while in other cases the site may be rejected due to complexity of the problems or higher costs of construction or long-term maintenance. Following is the summary of the main problems of Havasan dam based on the site investigation and related analysis which resulted in rejecting the site for dam construction.

Table 16 Discontinuities characteristics and the related intersection line in formation of unstable wedges for abutments

Joint set data			Sliding on intersection line	
Abutment	Joint set	Dip/dip direction (deg)	Dip/dip direction (deg)	Length (m)
Right	Bedding	63/075	25/359	359
	J1	41/302		
Left	Bedding	66/073	52/128	160.5
	J2	64/180		

Table 17 Output parameters for wedge analysis in the dam abutments

Parameter	Details	Right abutment	Left abutment
Wedge	Height (on slope) (m)	122.00	125.00
	Width (on upper face) (m)	185.03	4.75
	Volume (m ³)	625,684.00	562.47
	Weight (kg)	1.65E + 09	1.47E + 06
Force (kg)	Normal (joint1)	5.4E + 08	4.9E + 06
	Normal (joint2)	5.0E + 08	1.0E + 07
	Driving	9.6E + 08	0.0E + 00
	Resisting	8.5E + 08	0.0E + 00
Intersection angles (deg)	J1&J2 on slope face	63.71	2.60
	J1&Crest on slope face	60.04	76.40
	J1&Crest on upper face	109.57	84.02
	J2&Crest on slope face	56.25	101.00
	J2&Crest on upper face	35.03	35.14
	J1&2 on upper face	35.40	60.84

Table 18 Stability analysis of the right and left abutments for wedge failure (Rasouli Maleki 2010)

Filled with water (%)	Right abutment		Left abutment	
	Without earthquake loading–static	Earthquake loading–dynamic	Without earthquake loading–static	Earthquake loading–dynamic
0 (dry)	1.68	1.25	17.44	15.50
10	1.67	1.24	17.43	15.49
20	1.66	1.24	17.38	15.44
30	1.66	1.32	17.23	15.31
40	1.65	1.22	5.78	5.09
50	1.62	1.20	0	0
60	1.57	1.17	0	0
70	1.52	1.12	0	0
80	1.43	1.06	0	0
90	1.33	0.98	0	0
100 (saturated)	1.20	0.89	0	0

- Presence of clay-filled joints with apertures in excess of several centimeters in the right abutment of the dam could be one of the main factors for rejecting this site. There are two primary issues involved with clay-filled joints (Fig. 14):

(a) Escaping water from the reservoir could dislodge the clay infilling of the joints which has low to medium

liquid limit. Therefore, after filling of the dam the clay washout could cause some instability of the banks and abutments.

(b) Swelling pressure in clay layers impacts structural stability of the concrete dams, which are sensitive to deformation. Considering the movement of abutment

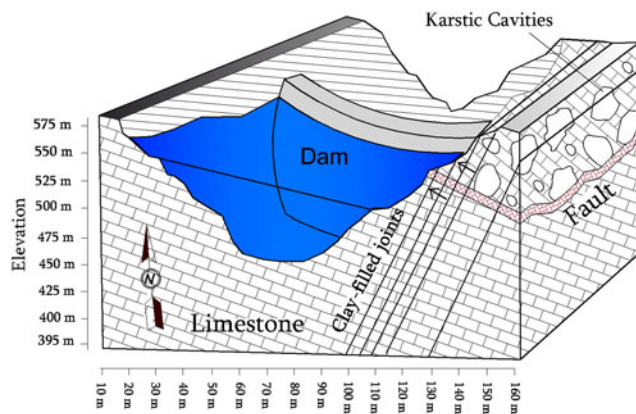


Fig. 14 Three-dimensional situation of clay-filled joints, fault, karstic cavities and trend of swelling pressure

and the results of swelling test and XRD for clay-filled joints which show the presence of swelling minerals such as illite and montmorillonite with low to medium swelling pressure, impounding of dam could cause swelling and finally lead to displacement of right bank. While the displacement could be in the range of millimeters, it could have major impact on structural integrity of the concrete dam.

- The presence of karstic springs located downstream and inside the reservoir and karstic structures which can cause severe leakage and water loss of the dam (Fig. 14). This leakage can lead to other performance and stability issues as will be discussed in following.
- Existence of faults below the design water elevation of the reservoir (Fig. 14). This combined with karstic conduits presents a big challenge on stabilizing the fault, since any stabilization measure requires changing the groundwater conditions within the fault and making the fault impermeable. Due to the size, location, and orientation of the fault zone relative to the abutments, this presents a major stability issue for the dam which could not be mitigated at reasonable costs to achieve the desired factor of safety.
- The high permeability of right bank based on the obtained results of in situ permeability tests such as Lugeon test in both banks. The results show higher permeability of right bank than of the left bank. Therefore, it is very likely that sealing this bank is another problem of the project, granted that other problems are addressed.
- Foundation stability of dam is questionable based on the results of DMR classification system. A quick review of the possible mitigation methods shows that the stabilizing measures are very costly and cannot provide the satisfactory factor of safety for the abutments and dam foundation.

- The unstable wedges in the banks of the dam could lead to dislodging of large blocks and filling reservoir of the dam and spillovers. In addition, it could decrease effective capacity of the dam and impose high maintenance costs in smaller scale. This refers to the fact that the slopes at the abutments could be stabilized by certain measures to assure the integrity of the concrete structure and spillways and related structures. However, the existence of these joints as a dominant structure along the reservoir banks should be considered in the assessment of long-term performance of the dam and their negative impacts quantified.
- The bedding conditions in banks and the high number of joint sets in the right banks indicate a high probability of plane failure on the banks and within the abutments. Meanwhile, the bedding dip and direction is suitable for water loss from the reservoir.

Therefore, along with other problems, it seems that the efforts required to stabilize the abutments and preventing the damage to the concrete structure will not be sufficient for a satisfactory long-term performance of the dam. It is due to the leakage and slope stability problems along the banks. In order to improve the selected Havasan dam site, if it is selected, more extensive investigations will be required to quantify some of the geological features accurately and enormous costs for mitigation shall be included. Given the ground conditions at the site, it seems that even at high costs of stabilizing the abutments and improving the foundation, the long-term performance of the site could be questionable. Thus, the site is rejected for dam construction, and it is recommended to look for other potential locations with less problematic site conditions, although the alternative locations may not be more attractive either from hydrological and topographical viewpoint.

10 Conclusions

Field investigations and petrographic analysis demonstrate that limestone (biocalcitic packstone) underlies the foundation and abutments of Havasan dam. The joint sets and fractures in right abutment are more extensive and more problematic than left abutment due to the effect of a fault zone. The rock masses of both abutments are heavily jointed with moderate spacing. Evaluation of the rock mass properties based on RMR, Q, GSI and DMR classification systems were performed and the results show that there are several stability and long-term performance issues involved with the foundations of the concrete structure as well as the banks of the reservoir.

The anticipated water seepage will be unacceptable due to the karstic conditions and open joints especially at the

right abutment (with aperture of over 70 mm). Therefore, the potential problems of slope stability, water seepage along with the presence of clay-filled joints in the dam site, swelling potential of clay infilling and pressures of 4.52–5.32 kPa have been considered in the evaluation of the site and subsequent decision to reject it.

Additional studies also show that even if the mitigation measures were to be used to stabilize the abutments and the foundation of the dam, sliding of rock blocks into the reservoir in the upstream due to plane failure of the slopes and resulting filling the reservoir could cause many long-term performance issues. The overall site investigation and subsequent analysis show that the construction of the dam will impose undue risks which could not be sufficiently addressed in the construction. One of them could be the possibility of dynamic loading which will cause unknown conditions. Thus, it was recommended to reject the site and look for alternative dam sites to utilize the water resources in the target area.

Acknowledgment The author is grateful to the M. Dousti, G. Barla, J. Rostami and F. Najafu for their help and cooperation in preparing the manuscript.

References

- Barton N, Bandis S (1990) Review of predictive capabilities of JRC–JCS mode; on engineering practice. Reprinted from: Barton NR, Stephansson O, Rock Joint Proc. of a regional conference of the international society for rock mechanics, pp 820
- Barton N (2000) TBM tunnelling in jointed and faulted rock. Rotterdam, Balkema, pp 169
- Barton N, Choubey VD (1977) The shear strength of rock joints in theory and practice. Rock mechanics. Springer-Verlag, no. 1/2, pp 1–54
- Barton NR, Lien R, Lunde J (1974) Engineering classification of rock masses for the design of tunnel support. *Int J Rock Mech* 4:189–239
- Bhasin R, Grimstad E (1996) The use of stress–strength relationships in the assessment of tunnel stability. *Tunn Undergr Space Technol* 11(1):93–98
- Bieniawski ZT (1989) Engineering rock mass classifications. Wiley, New York, p 251
- Grimstad E, Barton N (1993) Updating the Q-system for NMT. Proc. Int. Symposium on Sprayed Concrete, Fagernes, Norway, Norwegian Concrete Association, Oslo, pp 20
- Hoek E, Brown ET (1980) Underground excavations in rock. Institution of Mining and Metallurgy, London, p 527
- Hoek E, Brown ET (1998) Practical estimates of rock mass strength. *Int J Rock Mech Min Sci* 34(8):1165–1186
- Hoek E, Marinos P, Benissi M (1998) Applicability of the Geological Strength Index (GSI) classification for very weak and sheared rock masses. The case of the Athens Schist Formation. *Bull Engg Geol Env* 57(2):151–160
- ISRM (1981) Suggested methods for the quantitative description of discontinuities in rock masses. Rock characterization, testing and monitoring, London. Pergamon, Oxford, pp 221
- Jaeger JC, Cookm NGW (1969) Fundamentals of rock mechanics. Mathew and Co. Ltd., Section 3.4
- Mitri HS, Edrissi R, Henning J (1994) Finite element modeling of cable-bolted slopes in hard rock underground mines. SME Annual Meeting 14–17 February, New Mexico SME, Albuquerque, pp 94–116
- Ola SA (1982) Geotechnical properties of an Attapulgitic clay shale in Northwestern Nigeria. *Eng Geol* 19:1–13
- Ramana KV (1993) Humid tropical expansive soils of Trinidad: their geotechnical properties and areal distribution. *Eng Geol* 34:27–44
- Rasouli Maleki M (2010) Assessment of occurrence probability for planar and wedge failures under dynamic and static conditions in abutments of a double arch concrete dam (case study). 4th International Conference on Geotechnical Engineering and Soil Mechanics (ICGESM), Iran, p 520
- Rasouli Maleki, M (2011) Assessment and comparison of occurring probability of rock failures based on empirical and kinematical methods. 4th Iranian Rock Mechanics Conference (IRMC4), Tehran, pp 425
- Read SAL, Richards LR, Perrin ND (1999) Applicability of the Hoek–Brown failure criterion to New Zealand greywacke rocks. *Proceeding 9th International Society for Rock Mechanics*
- Rocscience (2002a) Dips user's guide. Rocscience Inc., Toronto, Ontario, Canada
- Rocscience (2002b) Swedge user's guide. Rocscience Inc., Toronto, Ontario, Canada
- Romana M (2003) DMR (Dam Mass Rating). An adaptation of RMR geomechanics classification for use in dam foundation. Inst. Cong. on Rock Mechanics. (Technology roadmap for rock mechanics) South African Inst. of Min and Met
- Seed HB, Woodward RH, Lundgren R (1962) Prediction of swelling potential for compacted clays. *J Soil Mech Found Div ASCE* 88(SM3):53–87
- Serafim JL, Pereira JP (1983) Considerations of the geomechanics classification of Bieniawski. *Proceedings international symposium engineering geology and underground construction*, vol 1. Balkema, Rotterdam, pp 1133–1142
- Singh B, Viladkar MN, Samadhiya NK, Mehrota VK (1997) Rock mass strength parameters mobilized in tunnels. *Tunn Undergr Space Technol* 12:147–154
- Snell and Knigth (1991) Susceptibility of dams to failure by sliding on sub-foundation strata that dips upstream. 17th ICOLD Vienna, Q66 R88